The Application of Porous Material in the Capillary Barrier System for Residual Soil Slope Stabilization

Nur Azlin Baharudin*, **Azman Kassim,**
Kamarudin Ahmad and Qurratu Aini Sirat

Department of Geotechnics and Transportation, School of Civil Engineering, Faculty Engineering,
Universiti Teknologi Malaysia, Skudai 81310, Johor, Malaysia

(***Corresponding author's e-mail: azmankassim@utm.my**)

Abstract

A drainage system that is used to flow excess rainfall infiltration is an excellent alternative to enhance lateral diversion capacity at the interface of Grade VI and Grade V soil slope layers thus delaying breakthrough occurrences. This study aims to explore the performance of porous transport layer on slope behavior via numerical simulation by GeoStudio SEEP/W. In this study, a 2-dimensional non-homogenous residual soil configuration model, which is composed of Grade VI and Grade V residual soil was constructed. Laboratory tests were conducted on the soil samples collected from the Faculty of Engineering, UTM JB to determine the soil properties as input parameters in numerical modeling. The soil slope model is designed as an infinite residual soil slope according to Jabatan Kerja Raya (JKR) design specification on the cut slope and fill slope with 27 ° inclination respectively. High rainfall intensities were chosen to represent rainfall infiltration in Johor. The slope model was modeled with a porous transport layer at the Grade VI and Grade V layer interfaces. The porous transport layer is introduced as the transport layer and its effectiveness is expected to be similar to the optimum compacted soil mix in the previous study. In addition, porous concrete as a transport layer is introduced and it must meet the adequate porosity and hydraulic conductivity requirements. The suction distribution pattern with depth and time was subsequently observed to identify the volume of infiltrated water and retention time in the transport layer. The porous transport layer is also expected to be efficient in diverting infiltrating water and decreasing the interface's suction distribution between Grade VI and Grade V soil layers.

Keywords: Porous concrete, Residual soil, Capillary barrier system, Soil slope, Slope stabilization

Introduction

The weathering process has resulted in soil heterogeneity, which is common to residual soil, and this type of soil accounts for more than 75 % of the surface deposits in Peninsular Malaysia [1,2]. Soil heterogeneities in tropical residual soil consist of weaker materials due to the weathering process. They affect the permeability of the soil mass thus controlling the mechanisms and locations of slope failure [3,4]. In Malaysia, the tropical climate with heavy rainfalls and high temperature facilitates a rapid chemical and mechanical weathering process resulting from a deep residual soil profile. The deep residual soil profile from various launches constitutes Grade VI and Grade V soils with clear strata interfaces in between the layers. The typical arrangement of soil layers is exhibited by the fine-grained soil near the soil surface compared to the soil in Grade VI and Grade V soils with distinct interfaces [5,6].

Several intrinsic and triggering factors influence the stability of residual soil slope. Characteristics such as soil composition, vegetation and slope gradient are the intrinsic factors, while the triggering factors include volcanic earthquakes and precipitation infiltration. Precipitation infiltration is one of the most important natural factors for slope instability in many parts of the world, especially in tropical climate regions covered with residual soils [7-10]. Damage caused by precipitation is usually shallow and damage not exceeding three meters is likely to occur on a 40 ° slope inclination. The suction effect of the soil matric suction decreases as the precipitation penetrates the soil and it is one of the failure mechanisms suggested by Zhang *et al.* [11]. Consequently, this would trigger a non-linear drop of soil shear strength. Hence, the matric suction of soil indicates near saturation soil resulting in slope stability that causes disasters such as landslides and debris flows.

The research method in this study involves the identification of optimum properties of the porous transport layer, which is layered with residual soils (Grade VI and Grade V). In this study, several important

parameters need to be taken into account such as the thickness of the fine-grained soil layer, the thickness properties of the porous transport layer and the inclination of Grade VI and Grade V soils with distinct interfaces as utilized in previous studies [12]. The thickness of the fined-grained soil layer is important for the optimum capillary barrier effect for the measurement of suction distribution. In addition, the thickness and hydraulic properties of the porous transport layer are the 2 main specifications for the development of the porous transport layer for optimum effectiveness. Meanwhile, the hydraulic properties of the porous transport layer include hydraulic conductivity and Soil Water Characteristic Curve (SWCC). These 2 parameters are decided from previous studies for an optimum application of transport layer in residual soil slope [12,13] The residual soil slope model inclination is also another important parameter as it gives a significant effect on the suction measurement.

The additional layer (porous transport layer, PTL) is made from coarse aggregate, fine aggregate, cement, and water to be sandwiched between Grade VI and Grade V soil layers. The design approach of the porous transport layer is mainly based on the proper selection of narrowly graded coarse aggregate and varying the paste volume until the target properties are achieved. Additionally, the water content and cement proportion that should be used in PTL are mainly based on the proportion of aggregate decided for the mix sample. The water-cement ratio (W/C ratio) and aggregate-cement ratio (A/C ratio) are applied to determine the water and cement proportion. High workability is regarded as one of the most important features of a sample. When a sample mixture does not crumble or becomes void free when squeezed and released, it is deemed to have high workability [14]. Balanced composition is also considered a successful mix design as it will result produce the best performance in terms of permeability, strength and durability. Besides, the continuity of cement paste with embedded coarse aggregate is the most important condition as the continuous voids would be maintained [15]. Generally, the A/C ratios are in the range of 4 to 6 by mass and aggregate contents between 1300 to 1800 kg/m^3. A higher ratio could reduce the strength of the mix sample [16,17].

Materials and methods

In this study, tropical soil samples were obtained from a slope within the campus of Universiti Teknologi Malaysia, UTM JB were used. The soil samples were collected from the study area and some of the samples were kept in moisture content containers for moisture content determination. The residual soil samples mainly consist of materials dominantly decomposed to Grade VI and Grade V. Data were obtained from representative soil to determine the index; engineering; mineralogical and hydraulic properties of the residual soils. The particle size distribution of the residual soil samples was determined by conducting wet sieving, dry sieving and hydrometer according to BS 1337: Part 2: 9.2, 9.3 and 9.5, respectively.

The purpose of Atterberg Limit tests is to identify the plastic limits and liquid limits of the residual soils. The procedures for this test are referred from BS 1377: Part 2: 1990: 4 and 5. The liquid limit of the soil samples was determined using a cone penetrator test. The small pycnometer method recommended in BS1377: Part 2: 1990 was referred for the determination of specific gravity (G_s) of the residual soil samples. The G_s is the ratio of soil density to the density of water. The following equation uses the specific gravity data to calculate other parameters such as the void ratio (e) and particle porosity (n).

$$e = \frac{G_s \gamma_w}{\gamma_d} \tag{1}$$

The porosity (n) of residual soil is described as the number of pore spaces in a soil mass and it is primarily influenced by the soil structure. The soil porosity was calculated from the void ratio (e), as follows:

$$n = \frac{1+e}{e} \tag{2}$$

The recommended procedure outlined in BS 1377: Part 4: 1990: 3.4 was applied to determine the maximum dry density (MDD) and optimum moisture content of the residual soil which are Grade VI and Grade V. A hydraulic conductivity test was conducted to determine the saturated permeability (k_{sat}) of the residual soils and the porous transport layer. The residual soils were examined by using falling head and the porous transport layer was tested by modified apparatus of the constant head method. The falling head method is generally recommended for fined-grained soil samples, whereas the constant head permeability test is generally recommended for coarse-grained soil samples [18]. These tests were performed in accordance with the procedure outlined in BS 1377: Part 5: 1990:5. However, to ascertain the accuracy of the results, a separate constant head test was performed with standard equipment. The results obtained from

the 2 methods were then compared to determine the most accurate result. The obtained data were then utilized as an input parameter in SEEP/W modelling to identify the hydraulic properties of the soil samples. The hydraulic properties for residual soils can be categorized into 2, namely Soil Water Characteristic Curve (SWCC) and unsaturated hydraulic conductivity function. The SWCC of the residual soils in this study were determined using pressure plate extractor tests, while the unsaturated hydraulic conductivity was predicted from various SWCC's as suggested by Singh and Kuriyan [19].

Development of porous material

Single-sized coarse aggregate grading between 9.5 and 19 mm is mainly used in the development of porous concrete [14]. Specifically, grading aggregate of 10 to 2 mm for coarse aggregate and grading 2 mm to 63 μm for fine aggregate. Portland cement and supplementary cementitious materials (SCMs) were used in the development of the porous transport layer as a binder. The physical and mechanical properties as well as chemical composition of the cement are the standards provided by the manufacturer. In this study, Ordinary Portland Cement was obtained from a local supplier in each mix with the specification given in AS (Australian Standard) 3972 - 1997. Meanwhile, the preparation of the standard porous concrete test specimen is based on the Australian Standards and Guidelines. The raw aggregate that has been sieved would be categorized into different groups using a standard sieve. Besides, the fine aggregate (sand) was also obtained from supplier. Water-cement ratio (W/C ratio) were kept constant at 0.4 in all mix designs. A standard tamping rod and proctor hammer were used to cast the porous transport layer cylinder for testing. Subsequently, control samples were cast using the consolidation technique used to cast conventional concrete cylinders, CSA A23.2-3C(I). According to CSA A23.2-3C(I) the concrete has to be cast in 3 layers with 25 stamps per layer. There are 2 types of mix proportions in this study which are TL1 and TL2 and the mix proportions are summarized in **Table 1**.

Table 1 Mix design of porous transport layer.

Description	Mix Proportion	
	TL 1	TL 2
Gravel (9.5 to 4.75) mm	50 %	75 %
Sand	50 %	25 %
W/C ratio	0.4	
A/C ratio	4	

Results and discussion

The 2-layered slope consists of Grade VI and Grade V residual soils from the 6-grade rock weathering classification system of the International Society of Rock Mechanics, ISRM (1981). Numerical modelling is the research approach employed in this study to achieve the objectives. In addition, preliminary data are necessary to ascertain the properties of residual soils through a detailed laboratory experiment. This section presents the preliminary data obtained from the laboratory testing of the representative soil sample of study area.

Index properties and soil classification

The index properties of the soils obtained in this study include the particle size distribution, Atterberg limits and specific gravity. Those properties were further used to classify the material based on British Standard Classification (BSCS). Grade VI and Grade V soils are both classified as clayey silt and gravelly silt. **Figure 1** shows the particle size distribution of Grade VI and Grade V through combined sieve analysis and hydrometer results. The soil materials, Grade VI and Grade V exist from the same parent rock due to the similar pattern of particle size distribution curve for both soils. The increased depth in the residual soil profile results in a decrease in the degree of weathering thus decreasing the fine content in the soil profile. The results show that the Grade V soil constitutes gravel, sand, silt and clay in different proportions while Grade VI shows a very low gravelly material with a high content of fine material. However, the Grade V residual soil has a coarse-grained content of 40.79% which is greater than the corresponding 7.63% of the Grade VI residual soil. Nonetheless, it is different from the fine content of Grade V of 49.5% which is lower than 91.9% of the fine material content of Grade VI. These findings are in good agreement with Yunusa and Kassim [12]; Kassim [13] on Grade VI and Grade V residual soils in FKE, UTM JB and Balai Cerapan

UTM JB. In general, the weathering process of residual soil is different for every study area, thus giving variations in the percentage of grain size and the type of mineral.

The moisture content of Grade VI is 46 % which is slightly higher than the moisture content of Grade V at 42 %. This may be attributed to the fact that the Grade VI residual soil layer is closer to the ground surface compared to Grade V therefore it is more often affected by variation in the flux boundary compared to the lower grade soil layer. Besides, the weathering process of residual soil decreases with depth and results in more fine content located near the surface hence the liquid limit of the Grade VI layer is higher than Grade V. The degree of weathering also influences the specific gravity of the soil sample according to Prondan and Arbanas [20]. Specific gravity is denoted indication density of minerals that make up the soil particles. The specific gravity for Grade VI and Grade V is 2.46 and 2.34, respectively Which implies that the density of mineral that forms Grade V is higher than Grade VI. In general, specific gravity increases as the variation of mineralogy increases.
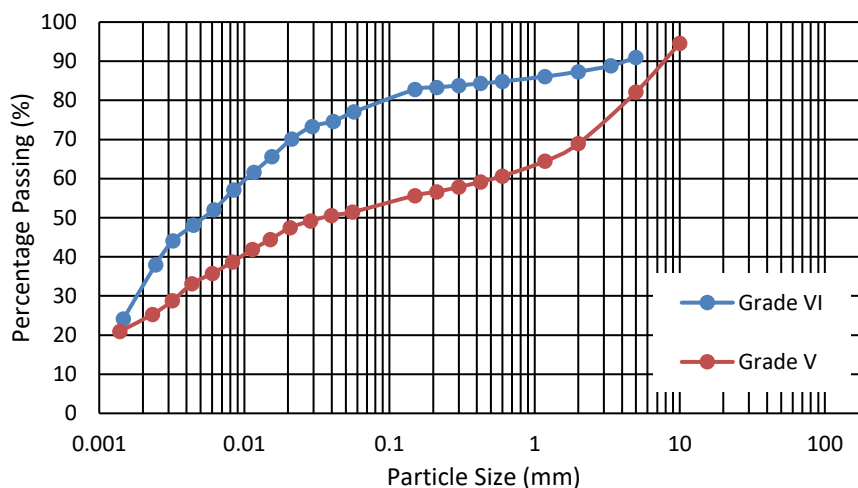

Figure 1 Particle size distribution of Grade VI and Grade V.

Soil sample engineering properties

The compaction test results for both soil samples, Grade VI and Grade V, are illustrated in **Table 2**. The compaction curve illustrates the identification of optimum moisture content (OMC) and maximum dry density (MDD). The density of Grade VI and Grade V for the laboratory soil model denotes a 90 % MDD at OMC. The test results (i.e. maximum dried density. ρ_d max and optimum moisture content) in this study are summarized **Table 2**.

Table 2 Summary of compaction test results for Grade VI and Grade V residual soils.

Soil	MDD (kN/m^3)	OMC (%)	Density of 90 % from MDD	Bulk density (kN/m^3)
Grade VI	13.27	29	11.94	15.41
Grade V	14.5	27	13.05	16.57

Shear strength properties

The shear strength characteristics of Grade VI and Grade V residual soils were determined through a uniaxial compression test. Soil specimens for both samples were prepared according to the 90 % of maximum dry density at optimum moisture content. Next, unconfined compressive strength (UCS) test was performed based on the recommended procedure outlined in BS 1377: Part 8: 1990:7. **Figure 2** shows the shearing stage (Stress Vs Axial Strain %) of Grade VI and Grade V residual soils. The output from the curve of the shearing stage depicts the identification of the Young Modulus (E) of the soil material for Grade VI and Grade V residual soils which has been used as an input parameter for the numerical modelling analysis.
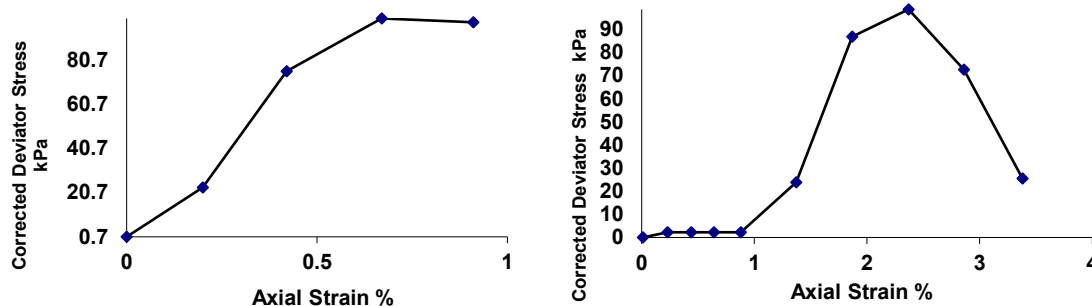
Figure 2 Shearing stage (Stress Vs Axial Strain %) of Grade VI and Grade V residual soil.

Permeability of Soil Sample (k_{sat})

The coefficient of saturated hydraulic conductivity is a quantitative measure of a saturated soil's ability to transmit water when subjected to a hydraulic gradient. It can be thought of as the ease with which pores of a saturated soil permit water movement. Evidently, the coefficient of Grade VI (1.01×10^{-8} m/s) is lower than Grade V (1.27×10^{-7} m/s) within 1 order magnitude which could be attributed to the smaller pore-sizes in Grade VI. In addition, the depth of soil layers influences the degree of weathering, which plays a significant role in the formation of residual soils. Soil layers near the ground are also expected to have more severe weathering and higher cumulative pore volume with a larger range of micro pore size distribution. Generally, the coefficient hydraulic conductivity for both soil materials in this study is within the soil range. The k_{sat} values also vary by several orders of magnitude due to changes in fabric, void fraction and water content, and they are also dependent on the clay content, sedimentation method, compaction energy level and compression rate. In summary, the k_{sat} value is influenced by the composition of soil grain, void ratio, arrangement of pores, condition of the soil, and the degree of compaction, including the form of water content, aggregation and the degree of saturation.

The k_{sat} values of Grade VI and Grade V are presented in **Table 3**. The results of a previous study by Yunusa and Kassim [12] of the k_{sat} value was used and elaborated on. For Grade VI residual soil, the k_{sat} obtained in the current study is 1.01×10^{-8} m/s which is lower than that of Yunusa and Kassim [12] with 5.89×10^{-7} m/s. Such a difference may be attributed to the variation in the fine material content because the clay content of Grade VI in the current study is 38 %, which is higher than that of Yunusa and Kassim [12] with 33 % [15]. On the other hand, the value of k_{sat} for Grade V residual soil obtained in the current this study is 1.23×10^{-7} m/s which is lower than that of Yunusa and Kassim [12] (i.e. 1.24×10^{-6} m/s) [15]. This difference, however, may be attributed to the variation in the gravel content of the studies. The gravel content recorded in the current study is 25.63 % while Yunusa and Kassim is 45 % [12].

Table 3 Summary of soil material properties used in the study.

Description	Residual soil	
	Grade VI: Clayey silt	**Grade V: Gravelly silt**
Composition		
Gravel (%)	2.12	25.63
Sand (%)	5.51	15.16
Silt (%)	53.9	28.5
Clay (%)	38	21
D60	0.013	0.6
D30	0.0019	0.003
D10	-	-
Moisture Content (%)	45.55	41.9
Liquid Limit (%)	89.67	83
Plastic Limit (%)	43.88	43.53

Description	Residual soil	
	Grade VI: Clayey silt	Grade V: Gravelly silt
Plasticity Index (PI)	39.12	46.14
Soil Classification		
Specific Gravity, Gs	2.46	2.34
Saturated Coefficient of -		
Permeability, ksat (m/s)	1.01E-08	1.23E-07
Bulk Density (kN/m3)	17.118	18.415
Dry Density (kN/m3)	11.943	13.050
Maximum Dry Density, MDD (Mg/m3)	13.270	14.500
Optimum moisture content, OMC (%)	29	27
Young modulus (kPa)	12620	25000

Hydraulic properties of residual soils and transport layer

The soil water characteristic curve (SWCC) and the unsaturated hydraulic conductivity represent the hydraulic properties of soil material. The results of the hydraulic properties are significant for the numerical modelling analysis in this study. Besides, the SWCC obtained from the hydraulic properties may be applied for laboratory modelling work as a reference for estimating the amount of water for soil mixing to be compacted in the 2-dimensional laboratory slope model and to achieve the target matric suction of the soil. The SWCC parameters were obtained through direct methods, namely pressure plate and axis translation technique employed in the laboratory test before determining the SWCC. In this technique, the pressure of the water phase (u_w), is maintained at the atmospheric level while the pore-air pressure (u_a), inside the apparatus is increased to desired pressure [21].

Soil Water Characteristic Curve (SWCC)

Figures 3(a) and **3(b)** show the SEEP/ W curve and fitted SWCC data of the soils in this study. There were 2 specimens for each of the soil samples tested to obtain the hydraulic properties and results. The particle size distribution has a significant impact on SWCC such that a larger particle size distribution increases the saturation of water content, which indicates a larger pore size of soil. As mentioned earlier, the laboratory data were determined from a series of pressure plate extractor tests performed on representative soil samples. Five pressures were applied on the pressure plate as an input parameter for further analysis as conducted by Fredlund and Xing in the SWRC Fit Web Interface [22,23]. The fitting values a, m and n were obtained to be applied as fitting parameters in the numerical modelling analysis. **Table 4** presents a summary of the results obtained from SWRC Fit.

Based on **Table 4**, Grade VI residual soil possesses a higher Air Entry Value (AEV) than other materials because it has more fine-grained material: hence it has a higher water retention capacity. Besides, the gravelly material with more coarse-grained material possesses lower AEV, which shows a lower retention capacity. Therefore, Grade VI residual soil with a higher AEV than Grade V residual soil has more capacity to store the infiltrating water and its lower residual water content will also allow for more moisture storage and transfer capacity.

Table 4 SWCC fitting parameter results for soil sample.

Soil type	Clayey silt	Gravelly silt	TL 1	TL 2
Saturated volumetric water content	0.725	0.669	0.2432	0.088
Air Entry Value, AEV (kPa)	0.700	0.590	0.21	0.09
Residual volumetric water content	0.30	0.20	0.087	0.084
Residual matric suction	28	21	0.09	0.06
Best-fitting parameters				
a	42.33	462.34	2.6192	1.9590
m	1.9	1.91	1.1246	0.8971
n	0.44	0.37	14.651	15.869

The pattern of SWCC depends on the pore size distribution between the materials [12,13]. In the case of Grade VI residual soil that contains more fine-grained material, the residual soil has a higher saturated volumetric water content than the gravelly soil which has more coarse-grained material. Therefore, Grade VI residual soil could retain more moisture with higher matric suction than other materials. Heidemann *et al.* [24] stated that the degree of weathering would not have a consistent effect on SWCCs [25]. Therefore, it is more likely that the parent rock type has a more significant influence on the SWCCs.

Suction-dependent hydraulic conductivity function

Figure 3 shows the hydraulic conductivity function of the soils from the SWCC. The hydraulic conductivity functions are predicted using Fredlund and Xing's method in SEEP/W. The figure shows the suction-dependent hydraulic conductivity function from the SWCC obtained from the pressure plate. The breakthrough suction was determined from the hydraulic conductivity curves of the soils intersection which indicates the capillary barrier effect. Two mix proportions were selected to be applied as the porous transport layer according to the hydraulic properties of the transport layer.
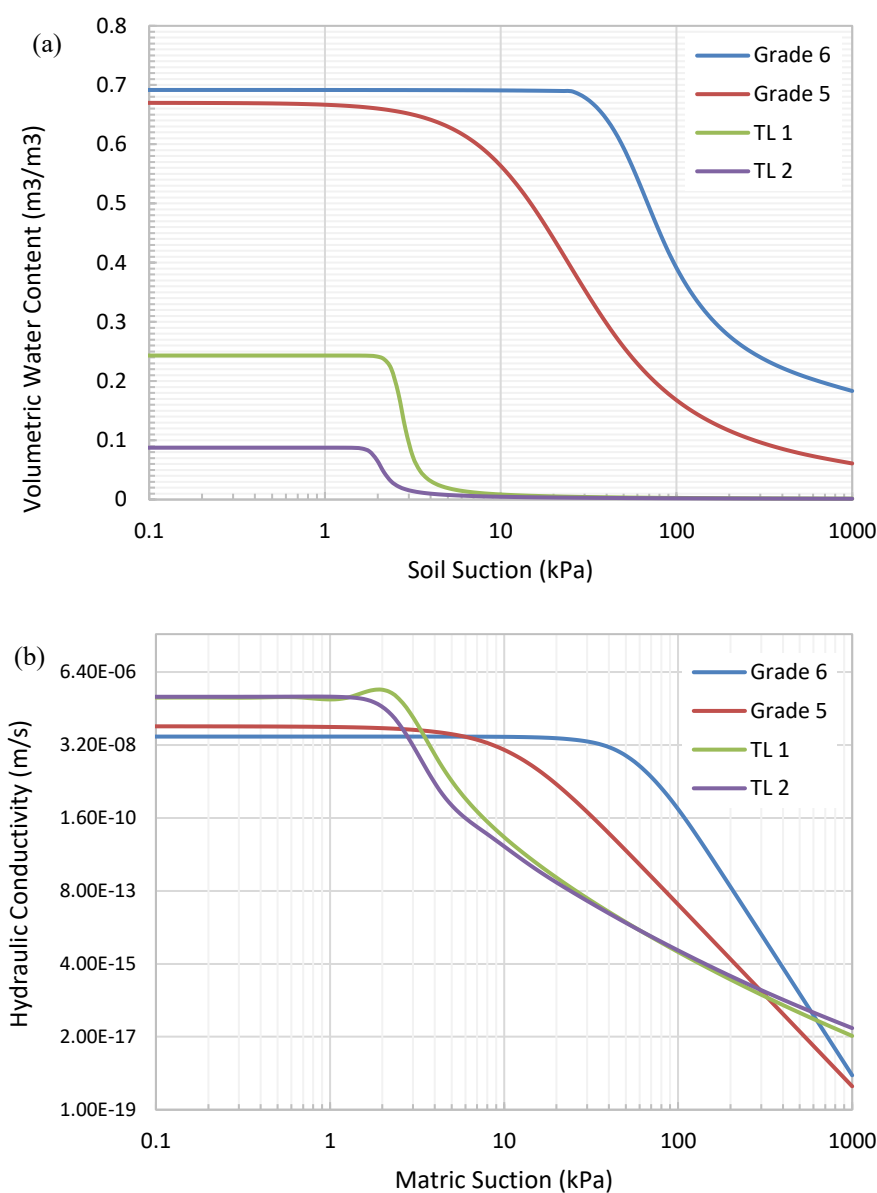

Figure 3 Hydraulic properties of residual soils and porous transport layer (a) SWCC (b) Hydraulic conductivity curve.

Numerical Simulation

Rainfall with high intensity (1.0586×10^{-5} m/s) was selected for this study including 4 and 24 h rainfall which are classified as high intensity with short duration. Results of the numerical simulation were presented and discussed in the form of matric suction versus depth and matric suction versus time to indicate the performance of porous material with the capillary barrier system. Matric suction versus depth shows the pattern of changes in pore water pressure with changes in the depth and advancement of the wetting front as rainfall continues to infiltrate into the slope. On the other hand, the results of pore water pressure versus time show the approximate time at which breakthrough occurs between each layer.

Suction distribution in 2-layered system without porous transport layer

The arrangement of the 2-layered system without the porous transport layer constitutes a clayey silt overlay with gravelly silt as the lower soil layer. However, the saturated hydraulic conductivity (k_{sat}) of both soil layers is not similar where the k_{sat} value of clayey silt is higher than gravelly silt. This illustrates that the gravelly silt soil layer has higher permeability than the clayey silt soil layer. This arrangement of soils is modelled in GeoStudio SEEP/W and subjected to high intensity rainfall patterns. These experiments would also generate suction profiles that are presented in the form of suction distribution with depth and suction distribution with time. The core of the experiment is to observe how the infiltrating water flows downward and eliminates the matric suction, while the latter was used to determine the breakthrough period. High intensity rainfall patterns were also used in the laboratory test to determine suction distribution with depth in a 2-layered slope without a porous transport layer.

The suction distribution for a 4 h rainfall pattern is presented in **Figure 4(a)**. The figure shows a uniform downward progression on infiltrating water at (0.1, 0.2 and 0.3) m soil profile depths. The contrast in soil properties between clayey silt and gravelly silt creates a capillary break, which results in the accumulation of infiltrating water above the interface. Besides, the increase in volumetric water content with time causes the accumulated water to flow laterally above the interface. The matric suction decreases at a 0.3 m depth with the increase in volumetric water content at the interface of the 2 soil layers. However, the matric suction at 0.42 m remained stable as the infiltrated water did not reach at the point.

Figure 4(b) presents the suction distribution of the 24 h rainfall pattern. The pattern of matric suction with depth at the early stage is similar to the 4 h rainfall pattern. A uniform downward progression of infiltrating water was observed at (0.1, 0.2, and 0.3) m depths. However, as rainfall continues, more water would infiltrate the clayey silt and accumulate above the soil layers interface. The matric suction at 0.42 m depth responded to the infiltrating water after 4 h of rainfall infiltration, which indicates the infiltrating water has percolated into the silty gravel. **Figure 4(bi)** shows the suction distribution with depth at the interface of clayey silt and gravelly silt.

The variations of matric suction with time due to 4 and 24 h rainfall patterns are presented in **Figure 5**. **Figure 5(a)** shows the variation of matric suction with time for the 4 h rainfall pattern. The matric suction increases instantaneously at the beginning of the rainfall event which signifies the accumulation of infiltrating water above the interface of clayey silt and gravelly silt soil layers. Perhaps, it does not penetrate the gravelly silt soil layers due to the capillary barrier effects influenced by the soil layer arrangement. The matric suction at the interface reaches approximately 15kPa which does not reach the breakthrough suction (6kPa) at the end of 4 h rainfall duration. This indicates no water infiltration into the gravelly silt soil layers, showing the water accumulation at the interface. **Figure 5(b)** shows matric suction with time for 24 h rainfall pattern. The matric suction decreased from the initial suction of 28 kPa until it reached the breakthrough suction after 6 h of rainfall infiltration. It became constant and uniform after 6 h which indicates water breakthrough occurrence into the gravelly silt soil layers unlike in the case of 4 h rainfall infiltration where the matric suction coincided with the breakthrough suction value after the breakthrough occurrence due to longer rainfall infiltration compared to the 4 h rainfall infiltration.
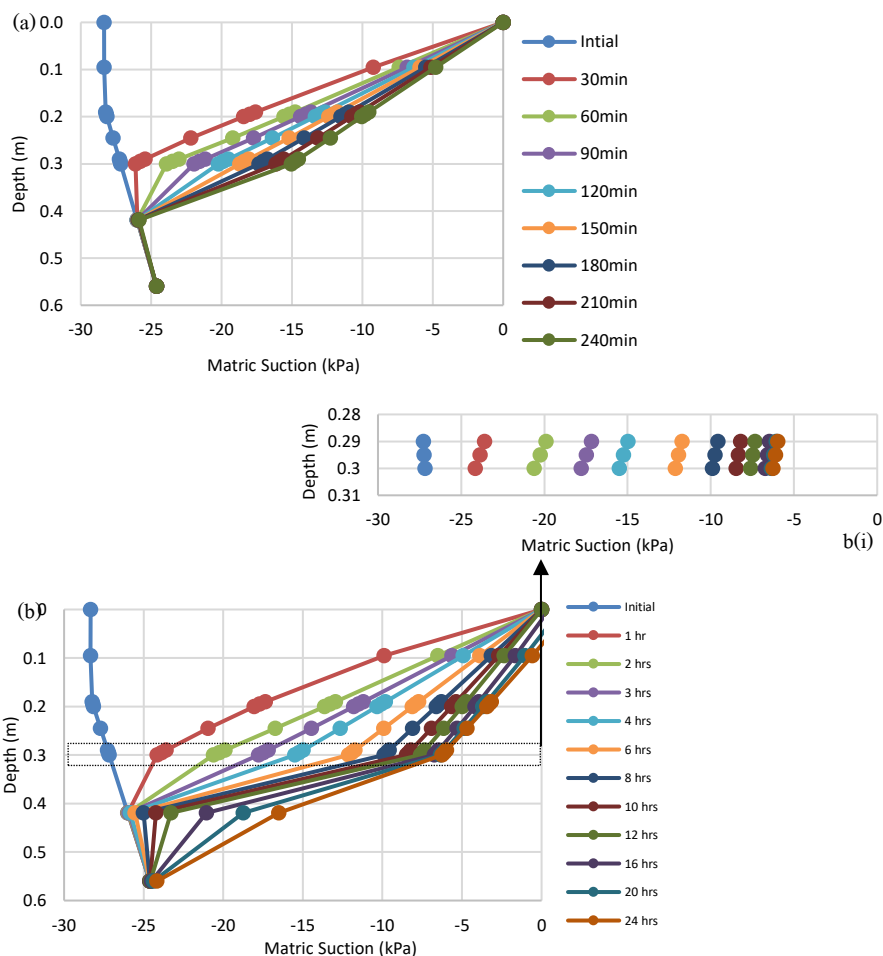
Figure 4 Suction distribution for clayey silt and gravelly silt without porous transport layer due to (a) 4 h and (b) 24 h rainfall pattern.
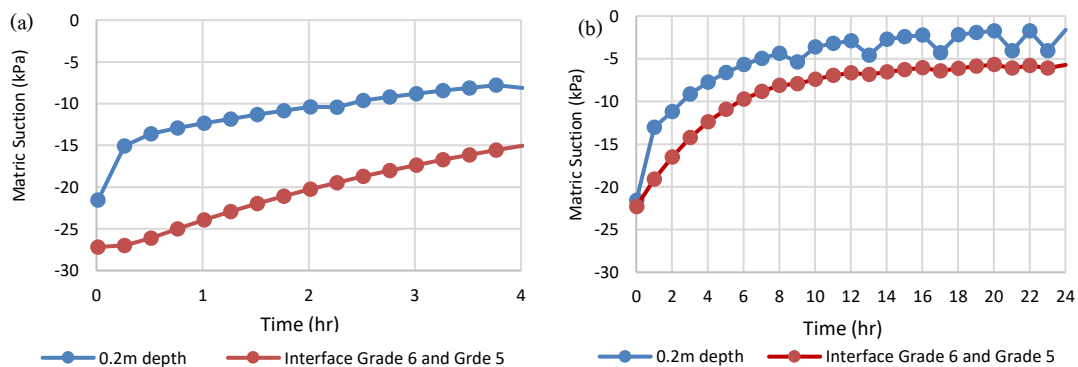

Figure 5 Suction distribution with time along the interface of clayey silt and gravelly silt due to (a) 4 h, (b) 24 h rainfall pattern.

Suction distribution in 2-layered system with porous transport layer 1

The previous section has discussed the suction distribution pattern in a 2-layered slope without a porous transport layer and the breakthrough occurrence in the gravelly silt. The breakthrough occurred only for 24 h rainfall pattern. In the subsequent discussions, 2 porous transport layers with different mix proportions and properties were applied as transport layers sandwiched in between clayey silt and gravelly silt soil layers (i.e at the interface).

In the first scheme, porous transport layer 1 (TL 1) was applied and located between clayey silt and gravelly silt soil layers. The initial 0.3 m thickness of clayey silt was changed to 0.2 m, while the remaining 0.1m serves as the thickness of TL1. The suction distribution with depth for high rainfall and medium rainfall patterns is presented in **Figure 6**. The suction distribution with depth due to the 4 h rainfall pattern is shown in **Figure 6(a)**. In general, the infiltrating water gives a uniform downward progression that is limited to (0.1 and 0.2) m depths. The infiltrating water further accumulates above the transport layer-clayey silt interface and is diverted laterally above the interface until reaches 60 min. Infiltrated water then seeps into the porous transport layer when it reaches 90min onwards. This is indicated by rapid variation in the matric suction at a 0.2 m depth due to an increase in the volumetric water content. Unlike the case of a 2-layered soil slope without a porous transport layer where the infiltrating water reached the depth of 0.45 m, infiltrating water for this scheme did not reach this depth. **Figure 6(bi)** shows detailed matric suction with depth at the interface.
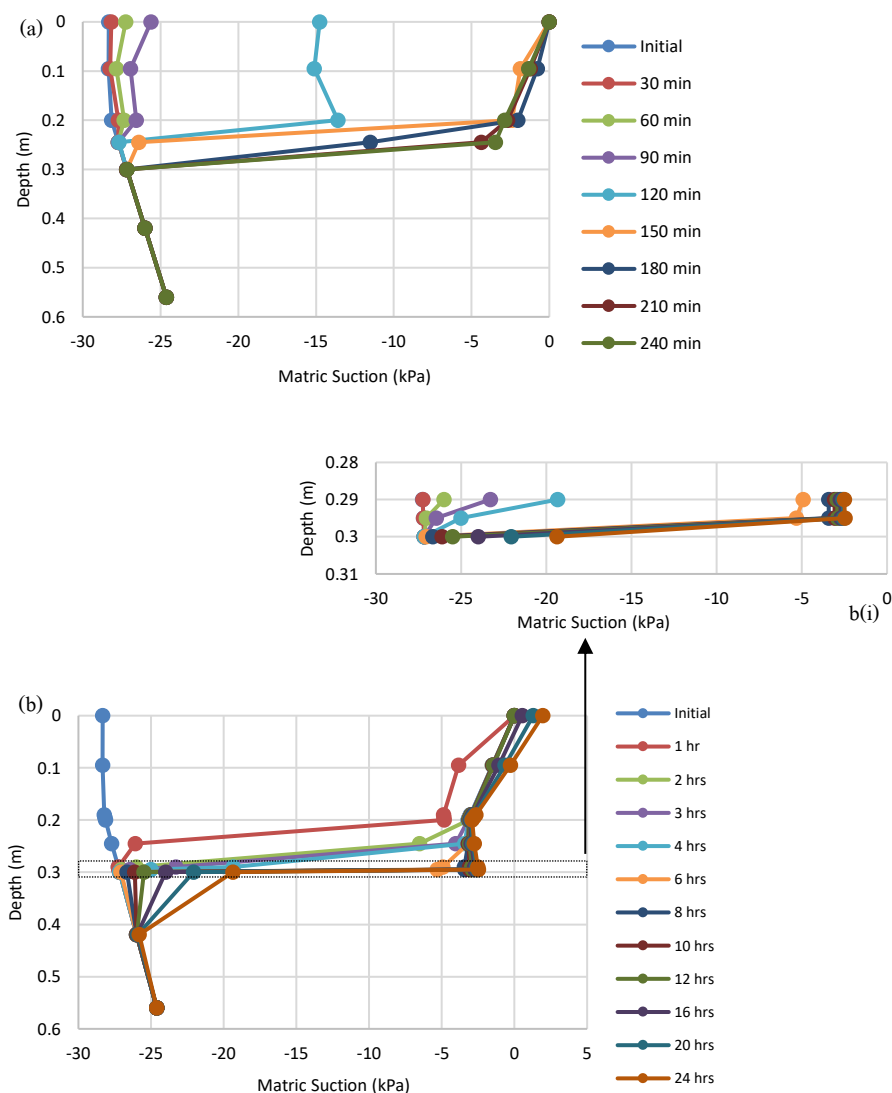

Figure 6 Suction distribution for clayey silt and gravelly silt with porous transport layer 1 due to (a) 4 h and (b) 24 h rainfall pattern.

For the 4 h rainfall pattern in **Figure 7(a)**, the matric suction increased at the beginning of the rainfall event which signifies the accumulation of infiltrating water above the interface of clayey silt and gravelly silt soil layers. Thus, it does not penetrate TL 1 due to the arrangement of layers between the transport layer and clayey silt. The matric suction at the interface between clayey silt and TL 1 reached breakthrough suction (1.8 kPa) approximately after 1 h of rainfall. However, the infiltrating water began to flow downward into TL 1 after 1 h of rainfall. This was observed in the suction distribution behavior, which became uniform after 1 h and increased beyond the breakthrough suction value. The suction distribution with time due to 24 h rainfall is presented in **Figure 7(b)**. Based on the figure, a significant amount of the infiltrating water was effectively diverted through the porous transport layer TL 1. The matric suction increased to 19 kPa which does not reach the breakthrough suction and remained constant until the end of the 24 h rainfall. As shown in the figure, the infiltrated water penetrating TL 1 is diverted and there was no water penetration from TL 1 to the gravelly silt soil layer. This is indicated by the decrease of matric suction and not reaching the breakthrough suction (1.5 kPa) at the interface between TL 1 and gravelly silt.
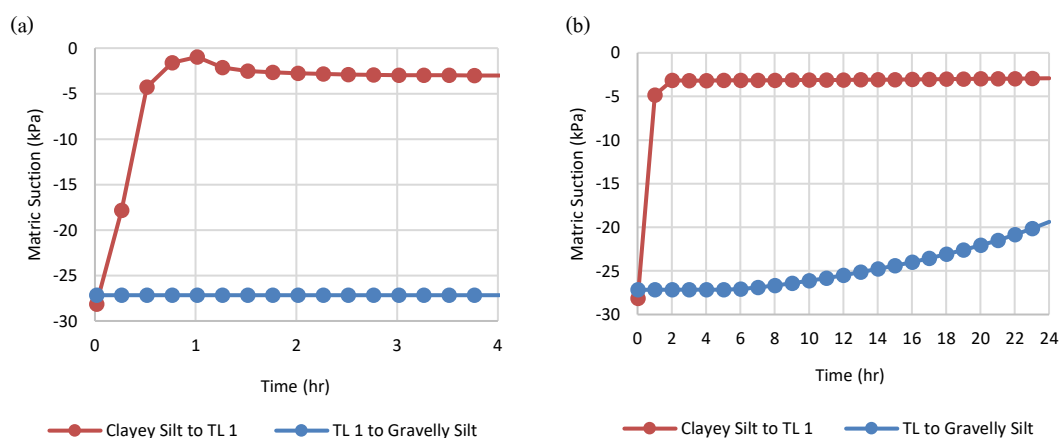

Figure 7 Suction distribution with time along the interface of clayey silt and TL 1 due to (a) 4 and (b) 24 h rainfall pattern.

Suction distribution in 2-layered system with porous transport layer 2

Figure 8 shows the suction distribution with depth for the 2-layered slope with porous transport layer 2 (TL 2) subjected to high intensity rainfall pattern. The suction distributions with depth for 4 h and 24 h rainfall patterns is presented in **Figures 8(a)** and **8(b)**, respectively. The figure shows a uniform progression of infiltrating water at 0.1 and 0.2 m depths (clayey silt soil layer). However, the infiltrating water was diverted above the porous transport layer-clayey silt interface until 2 h before percolation to the next layer due to the gap in soil properties between the 2 soil layers. This is evident from the rapid decrease in matric suction with time at 0.2 m depth due to an increase in the volumetric water content as rainfall infiltration continues. After 2 h of high-intensity rainfall, the infiltrating water started to penetrate the porous transport layer and was diverted through it. This can be observed from the decrease of matric suction at a 0.25 m depth towards the end of the rainfall duration. Furthermore, the matric suction at 2.5 m varies from 28 kPa at the beginning of the rainfall event to 2 kPa towards the end of the rainfall event.

The suction distribution due to 24 h rainfall pattern is presented in **Figure 8(b)**. The uniform downward progression of infiltrating water at 0.1 and 0. m depths of the clayey silt layer is due to the decreased matric suction as the volumetric water content increases. During the first 2 h of rainfall infiltration, there was a significant amount of infiltration in the clayey silt layer, resulting in the development of pore water pressure in the clayey silt layer. Perhaps, after 2.5 h of rainfall infiltration, the infiltrating water percolated the porous transport layer 2 (TL 2) and flow laterally. This can be observed from the decrease in matric suction from 28 to 23.4 kPa at a 0.3 m depth. There is no percolation of infiltration water to the gravelly silt layer as the matric suction was constant until the end of rainfall which is at a 0.42 m depth because the infiltrating water was impeded from percolating the gravelly silt soil layer due to the large contrast in particle sizes between porous transport layer 2 (TL 2) and gravelly silt.
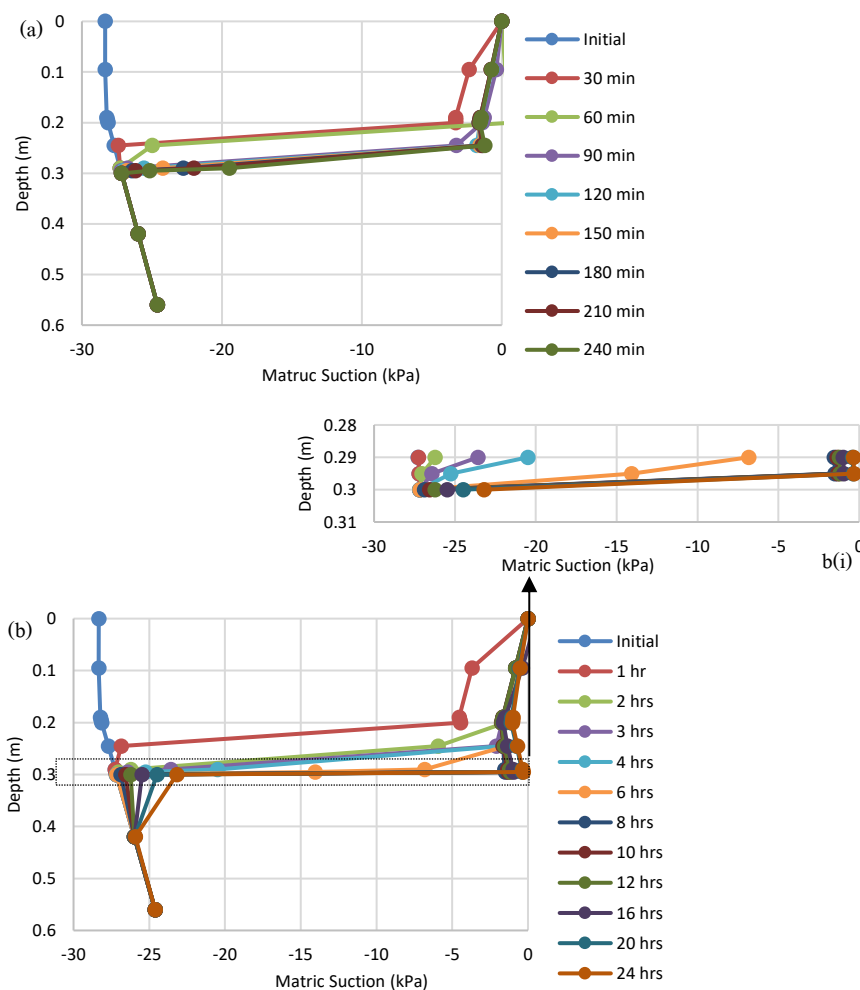
Figure 8 Suction distribution for clayey silt and gravelly silt with porous transport layer 2 due to (a) 4 h and (b) 24 h rainfall pattern.

For the 4 h rainfall pattern in **Figure 9(a)**, the matric suction increased at the beginning of the rainfall event which signifies the accumulation of infiltrating water above the interface of clayey silt and gravelly silt soil layers. Thus, it does not penetrate TL 2 due to the arrangement of layers between the transport layer and clayey silt. The matric suction at the interface between clayey silt and TL 2 reached breakthrough suction (1.8 kPa) after 1.5 h of rainfall. However, the infiltrating water began to flow downward into TL 2 after 1.5 h of rainfall. This was observed in the suction distribution behavior, which became uniform after 1.5 h and increased beyond the breakthrough suction value. The suction distribution with time due to 24 h rainfall is presented in **Figure 9(b)**. Based on the figure, a significant amount of infiltrating water was effectively diverted through the porous transport layer TL 2. The matric suction increased until it reached breakthrough suction approximately after 2 h of rainfall and remained constant until the end of the 24 h rainfall. Based on the figure, the infiltrated water that penetrates TL 2 was diverted and there was no water penetration from TL 2 to the gravelly silt soil layer. This is indicated by the decreased matric suction that does not reach the breakthrough suction (1.5 kPa) at the interface between TL 2 and gravelly silt.
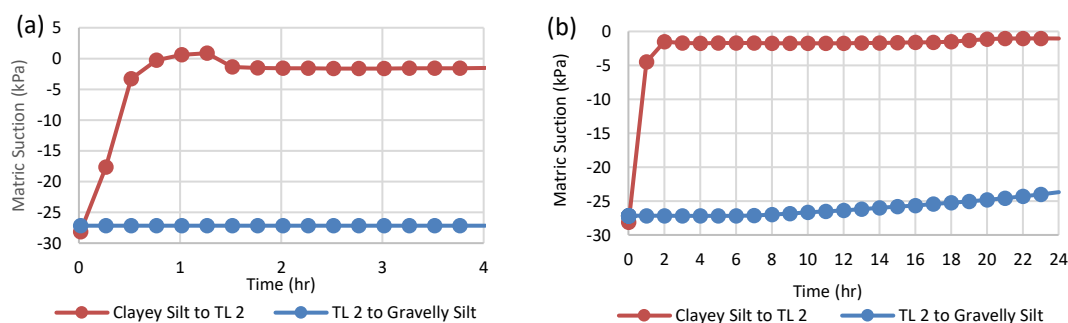
Figure 9 Suction distribution with time for clayey silt and gravelly silt with porous transport layer 2 due to (a) 4 h and (b) 24 h rainfall pattern.

Microstructure properties

The term 'microstructure' is used to describe the appearance of materials on the nanometer-centimeter length scale. The study on microstructure analysis supports the conclusion of the previous section. It is essential to notice that the performed microstructural analysis was qualitative and aims to give additional information for explaining the results.
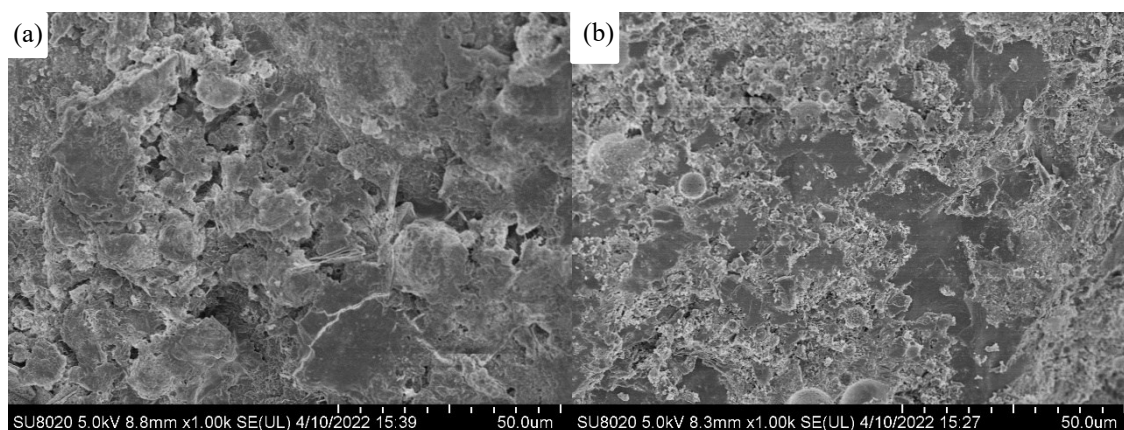

Figure 10 FESEM images of porous transport layer (a) TL 1 (b) TL 2.

Studies of the microstructure of cement paste and concrete have been primarily done using electron microscopy [26]. The FESEM images were obtained from the porous transport layer implemented between 2 layers of residual soils, clayey silt and gravelly silt. FESEM images of porous transport layers with different mix proportions namely TL 1 and TL 2 are shown in **Figures 10(a)** and **10(b)**, respectively. As the development of the porous transport layer progresses, the porosity of TL 1 is higher than TL 2 as expected and coincides with the hydraulic properties of each transport layer. This is because a porous transport layer developed with a higher gravel content would exhibit more pore compared to a higher sand content that would fill up the available void. The fine aggregates on effective porosity are not significant to the structure while coarse and complicated aggregates lead to more effective pores thus increasing permeability [27]. The smooth surface shown in both figures indicates the presence of gravel in both porous transport layers. As shown in previous studies, the gravel and sand possess cubicle particles with rough surfaces [12] and the dense and compact structure indicates better mechanical properties and higher strength of the structure [28]. The investigation also shows that microstructure influences the properties of concrete and that a strong correlation exists between the microstructural observations and the laboratory testing properties. Millogo and Morel [29] highlighted the importance of microstructural analysis and stated that the microstructure properties play important role in shaping the behavior of samples. The sample properties behavior should be tested and discussed from this perspective. In the current study, the microstructural properties analysis is significant as it is related to the permeability and strength of PTL. Besides, it has also been observed that analyzing the samples of microstructure characteristics can explain any previously unclear physical or mechanical behavior [30]. In this regard, electron microscopy presents a wide range of potential for assisting academics and working engineers in understanding soils.

Discussion

Over the last few years, the combined effort of academics and industrial scientists has resulted in numerous improvements to the residual soil slope stabilization method, including the advanced capillary barrier system with various improvements. The capillary barrier system for slope stabilization has been widely applied as its effectiveness has been proven. Its application has also been improved to control rainfall infiltration, thus affecting the negative pore water pressure within the unsaturated soil. Studies on contrast soil behavior provide a comprehensive understanding of the mechanisms of rainfall-induced slope failure. This also includes changes in the matric suction within unsaturated soil, which decreases as the volumetric water content increases because the water replaces the pore air pressure [31]. Passive measure in slope stabilization consists of maintaining and controlling rainfall infiltration. One of the passive slope stabilization measures is horizontal drain; however, the effectiveness is limited to diverting groundwater out of the slope, thus lowering the groundwater table [32]. This contradicts the application of the porous drainage layer, which lowers the volumetric water content at the slope surface, thus preventing the risk of shallow slope failure. Moreover, there are several studies on the application of capillary barrier cover with the transport layer being more effective than the conventional capillary barrier cover. The application of sand as transport material is also suggested as the particle size plays an important role in enhancing the capillary barrier effect [33,34]. For instance, a study on the long-term performance of capillary barrier with an unsaturated additional layer as drainage shows its effectiveness in diverting infiltrating rainfall in China's humid climate [34]. The development of positive pore-water pressure results in slope failure that is shallow in nature; therefore, the development of pore water pressure leads to slope failure and the poor drainage characteristics of the residual soil mantle can be improved significantly by introducing a transport layer.

Conclusions

In general, the performance of the porous transport layer in diverting the infiltrating water depends on the soil particle contrast between the soil layers which, in turn, affects the hydraulic properties of the material. An effective porous transport layer would help preserve the natural capillary barrier effects of the residual soil slope. The results obtained from the numerical analysis indicate that capillary break formed at the interface, impeding the downward water movement into the next layer of soil layers due to the contrast in particle size between both layers. The performance of porous material in a capillary barrier system for diverting infiltrated water was also studied and the system was subjected to the high rainfall intensities applied. Based on the outcome of this study, the following conclusion was drawn. Evidently, the results indicated that the capillary barrier effect exists in the 2-layered system of clayey silt and gravelly silt soil layers. The inclusion of a porous transport layer, which includes both mixed proportions of TL1 and TL2, has also modified the suction distribution behavior and sustained the natural capillary barrier system effect. Besides, TL1 was more effective in diverting water because the clayey silt layer possesses capillary forces due to a finer pore structure, thus increasing the ability to retain the infiltrating water. TL2 also diverted the infiltrating water; however, its diversion capacity is less than the TL1 porous transport layer due to the nature of its particle size. These findings are in good agreement with previous researchers that the higher the difference in the particle size contrast, the higher the percentage of water diversion [12].

Acknowledgements

References

[1]   P Saffari, W Nie, MM Noor, X Zhang and Q Liang. Characterization the geotechnical properties of a Malaysian granitic residual soil grade V. *IOP Conf. Ser. Earth Environ. Sci.* 2019; **289**, 012006.
[2]   MF Ishak, MF Zolkepli and M Affendy. Tropical residual soil properties on slopes. *Int. J. Eng. Tech. Sci.* 2017; **4**, 139-47.
[3]   SE Cho. Probabilistic stability analysis of rainfall-induced landslides considering spatial variability of permeability. *Eng. Geol.* 2014; **171**, 11-20.
[4]   HQ Dou, TC Han, XN Gong, ZY Qiu and ZN Li. Effects of the spatial variability of permeability on rainfall-induced landslides. *Eng. Geol.* 2015; **192**, 92-100.

[5]   JH Li, L Du, R Chen and LM Zhang. Numerical investigation of the performance of covers with capillary barrier effects. *S. Chin. Comput. Geotech.* 2013; **48**, 304-15

[6]   H Krisdani, H Rahardjo and EC Leong. Behaviour of capillary barrier system constructed using residual soil. *In*: Proceedings of the Geo-Frontiers Congress, Austin, Texas. 2005.

[7]   D Wang, L Li and Z Li. A regularized Lagrangian meshfree method for rainfall infiltration triggered slope failure analysis. *Eng. Anal. Bound. Elem.* 2014; **42**, 51-9.

[8]   AS Muntohar and HJ Liao. Rainfall infiltration: infinite slope model for landslides triggering by rainstorm. *Nat. Hazards.* 2010; **54**, 967-84.

[9]   LZ Wu, RQ Huang, Q Xu, LM Zhang and HL Li. Analysis of physical testing of rainfall-induced soil slope failures. *Environ. Earth Sci.* 2015; **73**, 8519-31.

[10] TL Tsai and SJ Chiang. Modeling of layered infinite slope failure triggered by rainfall. *Environ. Earth Sci.* 2013; **68**, 1429-34.

[11] GR Zhang, YJ Qian, ZC Wang and B Zhao. Analysis of rainfall infiltration law in unsaturated soil slope. *Sci. World J.* 2014; **2014**, 567250.

[12] GH Yunusa and A Kassim. Laboratory investigation of drainage cell as transport layer in residual soils. *Jurnal Teknologi* 2016; **78**, 6-12.

[13] A Kassim. 2011, Modelling the effect of heterogeneities on suction distribution behaviour in tropical residual soil. Ph. D. Dissertation. Universiti Teknologi Malaysia, Malaysia.

[14] American Concrete Institute. *Report on pervious concrete*. American Concrete Institute, Michigan, 2010.

[15] DS Patil, AM Khan and TAM Ansari. 2019, Experimental investigation on pervious concrete. Dissertation, Department of Civil Engineering, School of Civil Engineering and Technology, Anjuman-I-Islam's Kalkesar Technical Campus.

[16] P Chindaprasirt, S Hatanaka, T Chareerat, N Mishima and Y Yuasa. Cement paste characteristics and porous concrete properties. *Construct. Build. Mater.* 2008; **22**, 894-901.

[17] SB Singh, P Munjal and N Thammishetti. Role of water/cement ratio on strength development of cement mortar. *J. Build. Eng.* 2015; **4**, 94-100.

[18] IGB Indrawan, H Rahardjo and EC Leong. Effects of coarse-grained materials on properties of residual soil. *Eng. Geol.* 2006; **82**, 154-64.

[19] DN Singh and SJ Kuriyan. Estimation of unsaturated hydraulic conductivity using soil suction measurements obtained by an insertion tensiometer. *Can. Geotech. J.* 2003; **40**, 476-83.

[20] MV Prodan and Z Arbanas. Weathering influence on properties of siltstones from Istria, Croatia. *Adv. Mater. Sci. Eng.* 2016; **2016**, 1-15.

[21] M Wang, L Kong and M Zang. Effects of sample dimensions and shapes on measuring soil-water characteristic curves using pressure plate. *J. Rock Mech. Geotech. Eng.* 2015; **7**, 463-8.

[22] S Oh, YK Kim and JW Kim. A modified van Genuchten-Mualem model of hydraulic conductivity in Korean residual soils. *Water* 2015; **7**, 5487-502.

[23] YB Yamusa, MA Hezmi, K Ahmad, A Kassim, R Saari, N Alias and ASA Rashid. Soil water characteristic curves for laterite soil at different water contents and methods as lining system. *IOP Conf. Ser. Mater. Sci. Eng.* 2019; **527**, 012002.

[24] M Heidemann, LA Bressani, WYY Gehling, JAA Flores and MS Porto. Influence of structure in the soil-water characteristic curves of two residual soils of granite. *E3S Web Conf.* 2016; **9**, 11002.

[25] H Rahardjo, A Satyanaga, F Harnas, J Wang and E Leong. Capillary barrier system for landfill capping. *In*: Proceedings of the Coupled Phenomena in Environmental Geotechnics, Torino, Italy. 2013.

[26] PJM Monteiro, AP Kirchheim, S Chae, P Fischer, AA MacDowell, E Schaible and HR Wenk. Characterizing the nano and micro structure of concrete to improve its durability. *Cement Concr. Compos.* 2009; **31**, 577-84.

[27] J Hu, Z Qian, P Liu, D Wang and M Oeser. Investigation on the permeability of porous asphalt concrete based on microstructure analysis. *Int. J. Pave. Eng.* 2020; **21**, 1683-93.

[28] MIM Yusak, RP Jaya, MR Hainin and MH Wan. A review of microstructure properties of porous concrete pavement incorporating nano silica. *ARPN J. Eng. Appl. Sci.* 2016; **11**, 11832-5.

[29] Y Millogo and JC Morel. Microstructural characterization and mechanical properties of cement stabilized adobes. *Mater. Struct.* 2012; **45**, 1311-8.

[30] A Chegenizadeh, M Keramatikerman and H Nikraz. Importance of microstructural analysis in experimental soil stabilization. *Global J. Eng. Sci.* 2020; **4**, 1-4.

[31] MAM Ismail, NH Hamzah, NS Min, MHZ Abidin, SAA Tajudin and A Madun. Analysis of infiltration-suction response in unsaturated residual soil slope in Gelugor, Penang. *J. Phys. Conf. Ser.* 2018; **995**, 012052.

[32] H Rahardjo, V Santoso, E Leong, Y Ng, and C Hua. Performance of horizontal drains in residual soil slope. *Soils Found.* 2011; **15**, 437-47.

[33] TLT Zhan, H Li, GW, YM Chen and DG Fredlund. Physical and numerical study of lateral diversion by three-layer inclined capillary barrier covers under humid climatic conditions. *Can. Geotech. J.* 2014; **51**, 1438-48.

[34] L Zhan, W Jiou, L Kong and Y Chen. Long-term performance of capillary barrier cover with unsaturated drainage layer in humid climate. *In*: Proceedings of the Geo-Congress, Atlanta, Georgia. 2014, p. 1890-9.